Spherical-wave AVO-modeling in elastic and anelastic transversely isotropic (VTI) media

Arnim B. Haase and Chuck Ursenbach, CREWES, University of Calgary*

Summary

The AVO response of two-layer VTI models for AVO Class I is investigated. Graebner/Rueger reflection coefficients and the "Weyl-integral for anisotropic media" are utilized for the computation. Spherical wave results are compared with the plane-wave reflectivity. Depth dependence of spherical wave AVO is found to be strongest near critical angles, as was observed in the isotropic situation. Particle motion perpendicular to the ray angle is strongest just beyond critical angles and increasing with anisotropy. Anelasticity also modifies VTI AVO responses. When reflection amplitude losses due to attenuation are compensated for by unit reflectivity scaling, AVO-characteristics similar to the elastic situation are found. Q-factor dependence of spherical wave AVO is found to be strongest near critical angles. This Q-dependence, to some degree, mimics depth dependence of elastic comparisons. Particle motion perpendicular to the ray angle is also Q-factor dependent.

Introduction

Previous spherical wave AVO investigations by the authors are restricted to isotropic media (Haase, 2004; Haase and Ursenbach, 2004a). However it is well known that in many situations anisotropy is present either in the form of apparent anisotropy caused by layering or intrinsic anisotropy caused by, for example, shale layers. This type of anisotropy is usually called VTI (transversely isotropic with a vertical axis of symmetry). Rock fractures can cause HTI (horizontal symmetry axis TI) or also orthotropic anisotropy and these are not considered in this study.

Early work on spherical wave AVO by Hron et al. (1986) investigates anisotropy using asymptotic ray theory. They note that "anisotropic media produce noticeable differences in both amplitude- and time-distance curves as a function of the degree of anisotropy"; they also show amplitude-distance plots.

Previous work by the authors involved plane wave particle motion reflection coefficients given by Zoeppritz's equations and the Weyl/Sommerfeld integral for computing isotropic spherical-wave potentials. Plane-wave particle motion reflection coefficients for VTI media have been presented by Graebner (1992) and in refined form by Rueger (1996). The Weyl-integral for anisotropic media is given by Tsvankin (2001). Their "exact" equations are utilized in this study. Approximations are introduced by performing numerical integrations.

Q-factor dependence has also been observed in previous investigations of isotropic spherical-wave AVO (Haase, 2004; Haase and Ursenbach, 2004b). This modeling study seeks to quantify the sensitivity of spherical-wave AVO responses with respect to finite Q-factors of VTI media.

Theory

The displacement from a point force located at the origin is given by the following summation over plane waves (Tsvankin, 2001; equations 2.1-2)

$$\mathbf{u}(t,\mathbf{x}) = \frac{1}{2\pi}\int_{-\infty}^{\infty} \mathbf{S}(\omega,\mathbf{x})\Phi(\omega)e^{i\omega t}\,d\omega, \qquad (1)$$

$$\mathbf{S}(\omega,\mathbf{x}) = -\frac{i\omega}{4\pi^2}\sum_{\nu=1}^{3}\int_0^{\infty}\int_0^{2\pi}\mathbf{U}^{(\nu)}(\mathbf{p})\times e^{-i\omega\left[p_0 r\cos(\phi-\alpha)+p_3^{(\nu)}z\right]}p_0\,dp_0\,d\phi \qquad (2)$$

where $z = x_3$ is the vertical receiver coordinate, r is the horizontal offset, α is the source-receiver azimuth with respect to the x_1-axis, $\Phi(\omega)$ is the Fourier transform of the source pulse, $\mathbf{p}$ is the slowness vector with components $\{p_1 = p_0\cos\phi,\ p_2 = p_0\sin\phi,\ p_3\}$, and $\mathbf{U}^{(\nu)}$ is the displacement vector. For VTI media, there is no dependence on azimuth and the integration over $d\phi$ can be carried out analytically.

An explosive source (point source) can be modeled by three force pairs (Aki and Richards, 1980). Applying moment tensor methods leads, in cylindrical coordinates, to

$$S_r = \frac{iB\omega^2}{4\pi c_{33}c_{55}}\int_0^{\infty} R_{PP}(p_0)J_1(\omega p_0 r)e^{-i\omega\xi(z+h)}\times \frac{p_0^2\left[c_{55}p_0^2+(c_{33}-[c_{13}+c_{55}])\xi^2-\rho\right]}{\xi\left(\xi^2-\eta^2\right)}dp_0 \qquad (3)$$

$$S_\phi = 0$$

$$S_z = -\frac{B\omega^2}{4\pi c_{33}c_{55}}\int_0^{\infty} R_{PP}(p_0)J_0(\omega p_0 r)e^{-i\omega\xi(z+h)}\times \frac{p_0\left[(c_{11}-[c_{13}+c_{55}])p_0^2+c_{55}\xi^2-\rho\right]}{\left(\xi^2-\eta^2\right)}dp_0 \qquad (4)$$

where $R_{pp}(p_0)$ and the vertical slownesses ξ and η are given from plane-wave analysis (Graebner, 1992; Rueger, 1996).

The integrations shown in equations (3) and (4) compute particle motion, one frequency point at a time. Then we proceed as in the isotropic situation: When all frequency points have been computed for the desired output bandwidth, the time domain response is found by inverse Fourier transform, and quadrature traces are determined by Hilbert transform; from these two trace types spherical-wave amplitudes are calculated.

A mathematical treatment of anelasticity can be found in Aki and Richards (1980). They show that causality requires velocity dispersion and derive the following equation:

$$v(\omega) = v(\omega_{\text{ref}})\left[1 + \frac{1}{\pi Q}\ln\frac{\omega}{\omega_{\text{ref}}} - \frac{i}{2Q}\right] \qquad (5)$$

where Q is a frequency independent quality factor. Therefore, for anelastic models, velocities are complex and must be recomputed for every frequency point, according to equation (5).

Modeling

The same two-layer model as was utilized in the isotropic situation (Haase, 2004) is also employed in this study. The layer parameters are α_1 = 2000 m/s, β_1 = 879.88 m/s, ρ_1 = 2400 kg/m^3, α_2 = 2933.33 m/s, β_2 = 1882.29 m/s and ρ_2 = 2000 kg/m^3. As before, a 5/15-80\100 Ormsby wavelet is chosen as the source signature; a P-wave point source is assumed. VTI-type anisotropy of the top layer is introduced in two steps: weak anisotropy (ε = 0.15, δ = 0.05) and moderate anisotropy (ε = 0.3, δ = 0.1); the bottom layer is always assumed to be isotropic. VTI radiation patterns and free surface effects are ignored in this study.

For the anelastic situation, all layer velocities given above are considered to be 50 Hz reference velocities. Two values are assumed for the top layer P-wave quality factor: firstly, Q_{p1} = 100 and secondly, Q_{p1} = 387.5. The other Q-factors are calculated from α, β, and Q_{p1} utilizing empirical equations given by Waters (1978) and Udias (1999):

$$1/Q_P = \left(\frac{const.}{\alpha}\right)^2 \qquad (6)$$

$$Q_S = Q_P\,\frac{4}{3}\left(\frac{\beta}{\alpha}\right)^2 \qquad (7)$$

All Q-factors are considered to be isotropic in this study.

The appearance of the computed AVO results depends on scaling. Spherical spreading must be compensated for if results are to be compared to plane-wave responses. The Figures shown in this abstract give magnitude displays normalized to the response magnitude obtained when reflection coefficients R_{PP} in equations (3) and (4) are set to unity. Figure 1 compares AVO Class I spherical P-wave responses for weak and moderate VTI. Figure 2 shows anisotropic plane wave comparisons. Figure 3 demonstrates depth dependence of weak and moderate VTI spherical wave AVO. Q-dependence of weak and moderate VTI is displayed in Figures 4 and 5.
Particle Motion in these figures is taken to be in the ray direction. Figures 6, 7 and 8 give particle motion perpendicular to the ray direction for different Q-factors and degrees of VTI-type anisotropy. (Note the difference in vertical scale compared to Figures 1 through to 5.)

Discussion and Conclusions

Inspection of layer velocities given in the previous section shows an increase across the interface. Because of this velocity increase critical angles exist and head waves are generated for Class I AVO models. Increasing top layer VTI-type anisotropy decreases this velocity contrast and a shift of the critical point towards larger angles is expected. Figure 1 proves this to be the case. A similar shift can be observed in Figure 2, giving an anisotropic plane wave comparison. Note the indicated first zero crossing in these two AVO-magnitude displays. Increasing VTI-type anisotropy pushes this crossover point to ever higher angles for spherical waves, meaning the AVO gradient is decreasing for lower angles. For plane waves, by contrast, increasing VTI-type anisotropy moves the crossover point to ever smaller angles; the AVO gradient is increasing for angles below this point. The spherical wave VTI AVO depth dependence is displayed in Figure 3. For both weak and moderate anisotropy, larger depths "tweak" the AVO response near the critical point to lower angles toward a plane wave comparison. Similarly, VTI AVO responses are also "tweaked" by a change in Q-factors. Figures 4 (weak VTI) and 5 (moderate VTI) show a shift away from plane wave comparisons with decreasing Q-factors.

Normalized Q-dependence for spherical wave VTI AVO Class I, as given in Figures 4 and 5, to some degree mimics normalized depth dependence given in Figure 3. Increasing Q-factors and increasing depths move normalized spherical

wave VTI AVO closer to plane wave comparisons, as was observed in the isotropic situation.

In anisotropic materials particle motion is not in the propagation direction for P-waves or perpendicular to the propagation direction for S-waves. The terms used in the literature are quasi-P-waves (qP) and quasi-S-waves (qS). For the above displays the actual particle motion is projected onto the propagation direction (at the ray angle). Figures 6, 7 and 8 show the particle motion projection onto the ray angle normal for different Q-factors and degrees of VTI-type anisotropy. The maximum normalized displacement occurs just beyond critical points, where the head waves develop. This maximum displacement increases significantly with anisotropy. Q-factor dependence is similar to Figures 4 and 5 but is slightly larger.

References

Aki, K.T., and Richards, P.G., 1980, Quantitative Seismology: Theory and Methods: Vol. 1, W.H. Freeman and Co.

Graebner, M., 1992, Plane-wave reflection and transmission coefficients for a transversely isotropic solid: Geophysics, **57**, 1512-1519.

Haase, A.B., 2004, Spherical wave AVO modeling of converted waves in isotropic media: 74th Ann. Internat. Mtg. Soc. Expl. Geophys, 263-266.

Haase, A.B., and Ursenbach, C.P., 2004a, Spherical wave AVO-modelling in elastic isotropic media: CREWES Research Report, Volume **16**.

Haase, A.B., and Ursenbach, C.P., 2004b, Anelasticity and spherical wave AVO-modelling in isotropic media: CREWES Research Report, Volume **16**.

Hron, F., May, B.T., Covey, J.D., and Daley, P.F., 1986, Synthetic seismic sections for acoustic, elastic, anisotropic, and vertically inhomogeneous layered media: Geophysics, **51**, 710-735.

Rueger, A., 1996, Reflection coefficients and azimuthal AVO analysis in anisotropic media: Ph.D. Thesis, Colorado School of Mines.

Tsvankin, I., 2001, Seismic signatures and analysis of reflection data in anisotropic media: Pergamon.

Udias, A., 1999, Principles of seismology: Cambridge University Press, page 260.

Waters, K.H., 1978, Reflection Seismology: John Wiley and Sons, Inc., page 203.

Acknowledgements

Thank you to Professor E. Krebes for his help with the theory. Support by the CREWES team and its industrial sponsorship is gratefully acknowledged.

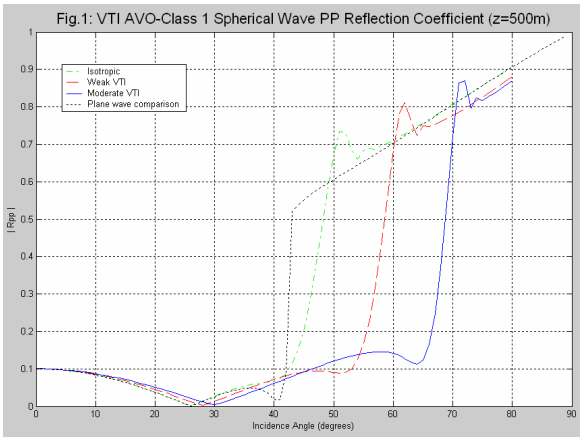

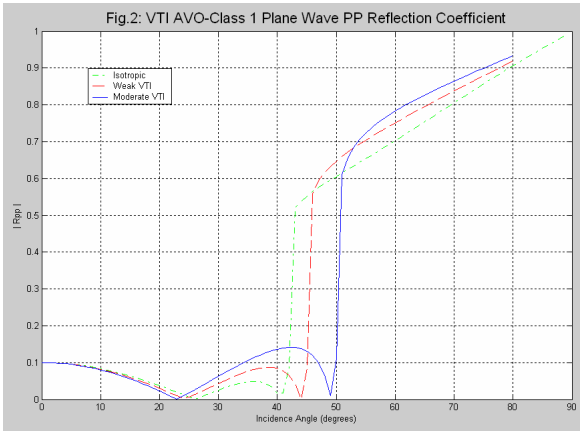

Spherical-wave AVO-modeling in VTI media